Role of Protein Cavities on Unfolding Volume Change and on Internal Dynamics under Pressure

Patrizia Cioni
Istituto di Biofisica, Consiglio Nazionale delle Ricerche, Pisa 56100, Italy

ABSTRACT The effects of two single point cavity forming mutations, F110S and I7S, on the unfolding volume change (ΔV^0) of azurin from *Pseudomonas aeruginosa* and on the internal dynamics of the protein fold under pressure were probed by the fluorescence and phosphorescence emission of Trp-48, deeply buried in the compact hydrophobic core of the macromolecule. Pressure-induced unfolding, monitored by the shift of the center of mass of the fluorescence spectrum, showed that ΔV^0 is in the range of 60–70 mL/mol, not significantly different between cavity mutants and compact azurin species such as the wild-type and the mutant C3A/C26A, in which the superficial disulphide has been removed. The lack of extra volume in F110S and I7S proves that the engineered cavities, 40 Å^3 in I7S and 100 Å^3 in F110S, are filled with water molecules. Changes in flexibility of the protein matrix around the chromophore were monitored by the intrinsic phosphorescence lifetime (τ_0). The application of pressure in the predenaturation range initially decreases the internal flexibility of azurin, the trend eventually reverting on approaching unfolding. The main difference between compact folds, wild-type and C3A/C26A, and cavity mutants is that the inversion point is powered from ~3 kbar to 1.5 kbar for F110S and <0.1 kbar for I7S, meaning that in the latter species pressure-induced internal hydration dominates very early over any compaction of the globular fold resulting from the reduction of internal free volume. The similar response between wild-type and the significantly less-stable C3A/C26A mutant suggests that thermodynamic stability per se is not the dominant factor regulating pressure-induced internal hydration of proteins.

INTRODUCTION

Close atomic packing in protein structures is an important determinant of the stability of native folds (1,2). The presence of internal cavities may be crucial, however, for conferring the conformational flexibility needed for their biological function. The extent to which naturally occurring or engineered cavities, sufficiently large to accommodate one or more water molecules, are empty or hydrated may depend on several factors (size, hydrophobicity, etc.) and is currently the subject of active debate (3–8). Unfortunately, internal mobile water molecules are not resolved by x-ray crystallography and neither by NMR spectroscopy, unless they are rotationally restrained (9). Some weakly polar cavities created inside proteins by mutations were indeed found to be empty (10) and studies of binding of noble gases within engineered cavities (7) have indicated that the occupancy of water in an apolar cavity is expected to be vanishingly small. Eriksson et al. (10) estimated that the probability of a single water molecule being in a purely hydrophobic cavity is extremely small, a conclusion strengthening the belief that absence of electron density in a crystallographic map is evidence for the absence of matter (9). However, free-energy considerations point out that empty cavities are very costly on stability, and recent x-ray, NMR, and simulation studies show that water molecules can be present, at least transiently (4,8,10–15).

One of the most sensitive approaches to the detection of internal cavities in macromolecules is the response of the system to applied pressure (16–19). When hydrostatic pressure is applied, the protein-solvent system evolves toward the global configuration that occupies the least volume (20). According to compressibility data (21–23), a decrease in volume can be achieved by both the reduction of internal cavities, voids that result from imperfect packing of amino acids, and greater hydration of the polypeptide, including the penetration of water molecules into the globular fold. (21,22,24). Since the major contribution to the change of volume on unfolding, ΔV^0, is the elimination of internal voids upon disruption of the folded structure, the introduction of an additional cavity of volume V_c should increase the value of ΔV^0 by roughly the same amount, were the cavity empty. Further, at predenaturating pressure reduction of cavity size and hydration exerts opposing influences on protein dynamics. From the correlation between compressibility, volume fluctuations, and flexibility (25) compression of cavities is expected to restrict the mobility of the polypeptide mainly of internal regions. Hydration, on the other hand, as it substitutes intrapeptide bonds with water bonds, will exert a lubricating action on segmental flexibility.

This works applies high pressure to a homogeneous series of proteins to enquire specifically on the extent to which relatively large internal cavities, created by the replacement of bulky side chains with smaller ones, may be empty or filled with water as well as on what is the influence of these cavities on pressure modulation of protein dynamics. Azurin from *Pseudomonas aeruginosa* was chosen as a model system for the wealth of structural (crystallographic, spectroscopic, and theoretical), thermodynamic, and kinetic data available on both native and mutated forms. Azurin is a 14 kDa

Submitted March 27, 2006, and accepted for publication June 12, 2006.

Address reprint requests to Patrizia Cioni, E-mail: patrizia.cioni@pi.ibf.cnr.it.

0006-3495/06/11/3390/07 $2.00

doi: 10.1529/biophysj.106.085670

copper-binding protein with an eight-stranded β-sandwich structure arranged in a double-wound Greek-key topology (26). The β-sandwich is closely packed and forms a highly hydrophobic core about the unique Trp residue (Trp-48) of the polypeptide (26,27), which serves as a natural probe of the local structure. The introduction of Ser in place of a bulky Phe (F110) or Ile (I7) creates in the neighborhood of Trp-48 a cavity of ~40 Å^3 in I7S and of 100 Å^3 in F110S, whereas for the rest the structure remains essentially native (28). The two single-point mutations destabilize the globular fold by 3–4 kcal/mole relative to the wild-type (WT) (29) and change the internal dynamics of the protein (30). A similar destabilization of azurin is observed upon severing the superficial C3-C26 disulfide link in the double mutant C3A/C26A (31), and for this reason the latter azurin species was taken to represent an example of compact but destabilized azurin fold.

The pressure unfolding equilibrium was monitored by the accompanying large change in fluorescence spectrum and yield of Trp-48, whereas the influence of pressure on the dynamics of the protein core was probed by phosphorescence lifetime of Trp-148 (32). For WT and the above azurin mutants, the phosphorescence emission of Trp-48 in copper free azurin is strong and long-lived even in buffer at ambient temperature (33), an emission that has proved to be remarkably sensitive to the flexibility of the structure surrounding the chromophore induced by a wide range of experimental conditions: metal binding (33), freezing (34), dehydration (35), high pressure (32), sugars (36), and pH (37).

The results of both stability and flexibility response to pressure demonstrate that water molecules do fill the nonpolar cavities of azurin and suggest that these hydrated cavities open the way to further internal hydration of the macromolecule, thus acting as nucleation sites for the unfolding process. The change in internal protein flexibility under pressure shows that with well compact protein folds, WT and C3A/C26A, the response is an initial enhancement of structural rigidity followed by a progressive loosening of the macromolecule in the high pressure range. The pressure at which there is an inversion between the two trends is apparently not related to the thermodynamic stability of the native state, but was found to be significantly lowered with the introduction of internal cavities effective in breaking up the compactness of the protein core.

MATERIALS AND METHODS

All chemicals were of the highest purity grade available from commercial sources. Water, doubly distilled over quartz, was purified by Milli-Q Plus system (Millipore, Bedford, MA). All glassware used for sample preparation was conditioned in advance by standing for 24 h in 10% HCl suprapur (Merck, Darmstadt, Germany).

Azurin WT and mutants I7S, F110S, and C3A/C26A were prepared following published protocols. The plasmid carrying the WT sequence was a generous gift from Prof. A. Desideri (Università di Roma, ''Tor Vergata'', Italy). The procedure of isolation and purification of WT has been described by van de Kamp et al. (38). Details about site-directed mutagenesis, protein expression, isolation, and purification of I7S, F110S, and C3A/C26A mutants have been described elsewhere (39,40). Copper free azurins (apoazurins) were prepared from holo-azurins by adding potassium cyanide and EDTA to final concentrations of 0.1 M potassium cyanide and 1 mM EDTA in 0.15 M Tris-HCl, pH 8, followed by column chromatography (38). The proteins were dialyzed and stored in Tris HCl, 10 mM, pH 7.5.

Equilibrium unfolding was analyzed according to the simple two-state ($N \leftrightarrow U$) model. The fraction of unfolded protein (f_U) was determined at each pressure from the displacement of the center of mass of the Trp fluorescence spectrum (29). Briefly, the center of spectral mass (ν) is defined as $\nu = (\Sigma \nu_i F_i)/(\Sigma F_i)$, where F_i is the fluorescence intensity at the wavenumber ν_i. f_U is related to ν by the expression

$$f_U = (1 + Q(\nu_p - \nu_U)/(\nu_N - \nu_p))^{-1},$$

where Q, the ratio of the quantum yields of unfolded and folded protein, is 0.3, $(\nu)_p$ is the center of spectral mass at each pressure, and ν_U and ν_N are the corresponding values for the unfolded and folded protein, respectively.

The free energy change, $\Delta G°$, was estimated from the linear plot

$$\Delta G = \Delta G° + p\Delta V^0,$$

where

$$\Delta G = -RT \ln K = -RT \ln (f_U/f_N).$$

Sample preparation for phosphorescence measurements

Before luminescence measurements, all proteins were extensively dialyzed in Tris-HCl (2 mM, pH 7.5) whose pH is one of the least sensitive to pressure. For phosphorescence measurements, it is paramount to rid the solution of all O_2 traces. Deoxygenation of protein samples was obtained by adding an enzymatic system composed of 80 nM glucose oxidase, 16 nM catalase, and 0.3% (w/v) glucose. No emission from these proteins could be detected at the amplification levels of phosphorescence measurements. The protein concentration in all phosphorescence experiments ranged between 2 and 4 μM.

Luminescence measurements

Fluorescence spectra and phosphorescence spectra and decays were measured with pulsed excitation ($\lambda_{ex} = 292$ nm) on a homemade apparatus (41), modified to implement spectral measurements by means of a charge-coupled device (CCD) camera. The main advantages of CCD detection over the traditional scanning monochromator-photomultiplier assembly are enhanced sensitivity to low light levels (>100-fold) and simultaneous acquisition of the entire spectrum.

Pulsed excitation was provided by a frequency-doubled Nd/Yag-pumped dye laser (Quanta Systems, Milan, Italy) with pulse duration of 5 ns, pulse frequency up to 10 Hz, and energy per pulse varying from 10 to 1000 μJ. For spectra measurements, the emission was collected at 90° from the excitation and dispersed by a 0.3 m focal length triple grating imaging spectrograph (SpectraPro-2300i, Acton Research, Acton, MA) with a band pass ranging from 1.0 to 0.2 nm. The emission was monitored by a back-illuminated 1340 × 400 pixels CCD camera (Princeton Instruments Spec-10:400B (XTE), Roper Scientific, Trenton, NJ) cooled to −80°C. Phosphorescence decays were monitored by collecting the emission at 90° from vertical excitation through a filter combination with a transmission window of 405–445 nm (WG405, Lot-Oriel, Milan Italy; plus interference filter DT-Blau, Balzer, Milan, Italy). A gating circuit that inverts the polarity of dynodes 1 and 3, for up to 1.5 ms after the laser pulse, protects the photomultiplier (Hamamatsu R928, Hamamatsu City, Japan) from the intense fluorescence light pulse.

The photocurrent was amplified by a current-to-voltage converter (SR570, Stanford Research Systems, Stanford, CA) and digitized by a 16 bits high

speed (1.25 MHz) multi-function data acquisition board (NI 6250 PCI, National Instrument Italy, Milan, Italy) supported by LabVIEW software capable of averaging multiple sweeps. Prompt fluorescence was collected through a 310–375 band pass filter combination (WG305 nm plus Schott UG11) and detected by an ultraviolet-enhanced photodiode (OSD100-7, Centronics, Newbury Park, CA).

An analog circuit was used to integrate the photocurrent, and its output was digitized and averaged by a multifunctional board (PCI-20428, Intelligent Instrumentation, Tucson, AZ) utilizing LabVIEW software. The prompt fluorescence intensity was used to account for possible variations in the laser output between measurements as well as to obtain fluorescence-normalized phosphorescence intensities. All phosphorescence decays were analyzed in terms of a sum of exponential components by a nonlinear least-squares fitting algorithm (DAS6, Fluorescence decay analysis software, Horiba Jobin Yvon, Milan, Italy).

Each spectral and lifetime determination was repeated at least three times.

Luminescence measurements under pressure were carried out by placing the sample cuvette in a pressure cell (SITEC, Zurich, Switzerland) provided with sapphire windows and employing water as pressurizing fluid. Details of the sample cuvette and procedure to avoid O_2 inlet during pressure cycles have been reported before (32). The reversibility of luminescence measurements was checked at the end of each pressure cycle. Particular care was taken to assure temperature equilibration of the sample after each pressure variation, which required at least 5 min.

RESULT AND DISCUSSION

Effects of internal cavities on the unfolding ΔV^0

The volume change of azurin denaturation was obtained from the linear relationship describing the pressure dependence of the unfolding free energy, $\Delta G(p) = \Delta G^\circ + p\,\Delta V^\circ$, where p is the applied pressure(42). At any p, the fraction of unfolded azurin, f_U, was determined from the change in the fluorescence emission, spectrum and quantum yield, of the single Trp residue (W48) buried in the central hydrophobic core of the macromolecule. The nonpolar rigid environment confers to W48 the bluest and most structured spectrum reported to date in proteins, a feature particularly suitable for distinguishing native from unfolded states of the macromolecule. Fig. 1 shows the large red shift, λ_{max}, increasing from 308 to 355 nm, and the decrease in fluorescence yield accompanying pressure denaturation of WT azurin. The spectral change is similar to that found with chemical denaturation by GdnHCl (29,36) and is typical for the full exposure of the aromatic residue to the solvent. Note that relative to WT and the mutant C3A/C26A, the fluorescence spectrum of mutants I7S and F110S is partially red-shifted and less resolved (39), an indication that the environment of W48 has been modified by the amino acid substitution. For each protein, f_U as function of applied pressure was evaluated from the change in the center of mass of the spectrum, λg, as described in Materials and Methods.

Pressure denaturation of azurin was found to be a reversible process, although for the cavity mutants recovery of the native fold is not immediate nor complete on decompression, particularly if the sample is maintained for a long time, over 20–30 min, at denaturing pressures. Evidently, for these proteins, slow, partly irreversible processes set in with

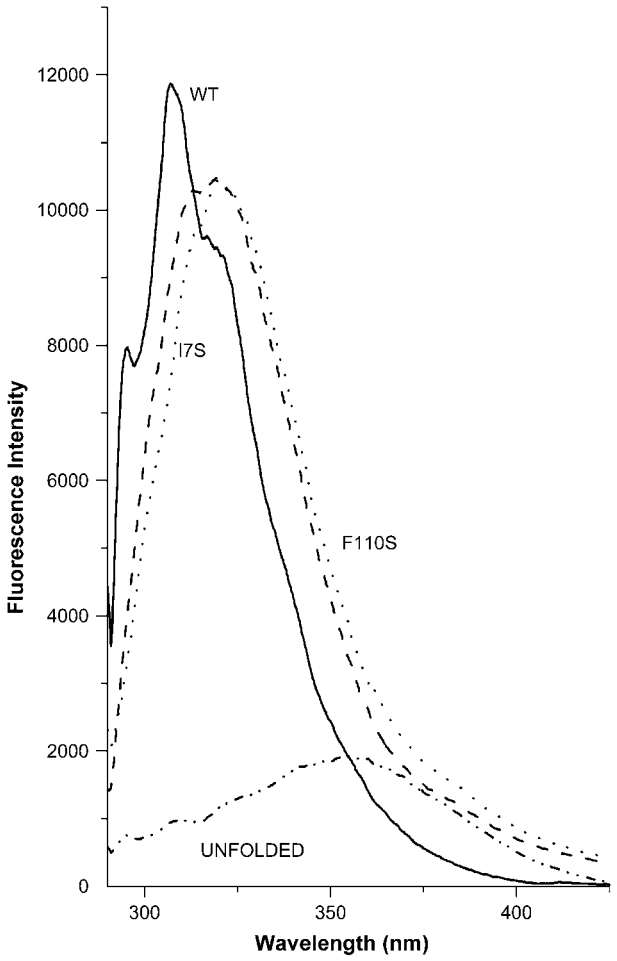

FIGURE 1 Fluorescence spectrum of native (*solid line*), F110S (*dotted line*), I7S (*dashed line*), and pressure unfolded (7 kbar) (*dash-dotted line*) apo azurin in Tris Cl 2 mM, pH 7.5. λ_{ex} was 292 nm. The spectrum of mutant C3A/C26A is the same as that of WT. The protein concentration was 2 μM.

the formation of denatured species. The phenomenon is not concentration-dependent, indicating that aggregation of protein is not responsible of it. To minimize the interference of these side reactions on the unfolding equilibrium, the time of equilibration after each pressure change was reduced to 5 min and the equilibration kinetics accelerated by raising the temperature to 40°C. Specific tests confirmed that under these conditions, recovery of native azurin at the end of a complete pressure cycle was better than 90%.

The pressure profiles of the denatured fraction, f_U, are shown in Fig. 2. Relative to the WT, the sensitivity to pressure denaturation is drastically enhanced in all mutant proteins, $P_{1/2}$ decreasing from ~6 to 1.1–1.5 kbar. Assuming a two-state process, the equilibrium constant is calculated from primary data according to

$$K(p) = f_U/f_N = K(0)\exp(-p\Delta V^\circ),$$

where $K(0)$ is the equilibrium constant at atmospheric pressure, ΔV° is the standard volume change of unfolding,

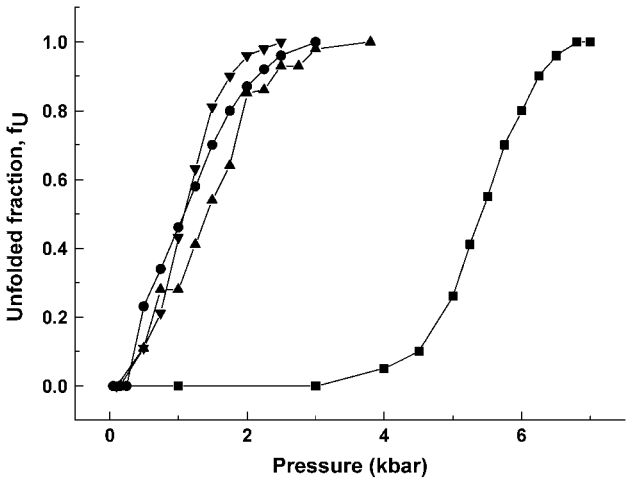

FIGURE 2 Pressure denaturation profile of azurin WT and mutant forms in Tris Cl 2 mM, pH 7.5, at 40°C. WT (■), F110S (▼), I7S (▲), and C3A/C26A (●). Each point is the average of at least three independent experiments. Other experimental conditions are as in Fig. 1.

and $\Delta G^\circ = -RT\ln K(0)$ is the free energy change at atmospheric pressure. The values of ΔG° and ΔV° obtained for the four azurins are collected in Table 1. Rather unexpectedly, the results point out that ΔV° is roughly the same with each protein, and show that the instability to pressure denaturation of the mutants is owed predominantly to their 3–4 times smaller stability (ΔG°) relative to the WT. We note that all free-energy changes, but that of WT, extrapolated from the pressure denaturation profile are ~1 kcal/mole smaller than the values obtained from denaturation in GdnHCl at 20°C (36) (see Table 1). Considering that pressure data refers to 40°C, where the mutant proteins are less stable, the agreement with chemical denaturation is rather satisfactory. In the case of the WT, the high denaturation pressure can give rise to a large error in the determination of ΔG° by the long extrapolation to atmospheric pressure. A previous study (29) limited to a pressure range of 2.6 kbar reported values of ΔV of unfolding of WT, F110S, and I7S significantly smaller than those reported here. It is evident that the pressure range spanned in that study is insufficient to denature the WT protein and therefore to compare the value of ΔV between WT and cavity mutants.

The main conclusion from the pressure denaturation profile is that the volume change on azurin unfolding is not significantly different between compact globular folds, WT, and C3A/C26A mutant, species in which a sizable internal cavity was introduced by the amino acid replacement.

TABLE 1 Unfolding free energy and volume change values relative to the denaturation of azurin species by high pressure at 40°C

Protein	ΔG^0 (kcal/mole)	ΔV^0 (mL/mole)
WT	8.6 ± 1.0	60 ± 10
C3A/C26A	1.8 ± 0.4	58 ± 9
F110S	2.2 ± 0.4	75 ± 11
I7S	2.2 ± 0.4	64 ± 10

TABLE 2 Typical lifetimes and relative amplitudes derived from a biexponential fitting of the phosphorescence decay of WT and mutants azurins

Protein	τ_1(s)	τ_2(s)	α_1
WT	0.12	–	1
C3A/C26A	0.1	–	1
F110S	0.23	0.07	0.04
I7S	0.029	0.02	0.25

The crystallographic structure of the two azurin cavity mutants I7S and F110S shows that by replacing I7 or F110 with the smaller and polar Ser, a predominantly hydrophobic cavity of ~24 and 60 mL/mole, respectively, has been engineered in proximity of Trp-48 (28), with important consequences on the stability and internal dynamics of azurin (29,30). In contrast to I7S, where no water molecules have been detected in the cavity, one water molecule sufficiently structured to give a diffraction pattern was indeed detected in the cavity of F110S (28). However, since the larger cavity of F110S can in principle accommodate 7–8 water molecules, x-ray data could be interpreted to mean that in both mutants the cavities are largely empty.

The increments to the total volume change measured for the mutants by x-ray measurements are significantly larger than the experimental error of ΔV° (~10 mL/mole) and therefore were the cavities empty would show a 40% and 100% increase of ΔV°, respectively. We must infer that the cavities are largely filled with water.

Effects of internal cavities on the response of protein dynamics to applied pressure

The application of high pressure will promote any structural rearrangement of the macromolecule/solvent system that accommodates a reduction in its volume. At predenaturating pressures, the decrease in volume can involve both the reduction of internal cavities and greater hydration of the polypeptide, including the penetration of water molecules into the globular fold. Cavity size reduction and hydration exert opposing influences on protein dynamics, and the net effect will manifest which of the two trends is the prevailing structural adaptation to applied pressure.

The internal dynamics of azurin is assessed by the phosphorescence lifetime of W48 (τ_0), a parameter whose magnitude depends directly on the flexibility of the protein matrix around the chromophore (43,44). In buffer (2 mM Tris, pH 7.5) at 40°C, the phosphorescence decay of W48 in WT azurin and in the C3A/C26A double mutant is uniform with a lifetime of 0.12 and 0.10 s, respectively. For the cavity-forming mutants F110S and I7S, the decay is heterogeneous, reflecting the presence of more than one stable conformation of the macromolecule in the millisecond-second timescale, each with its own τ (30) (Table 2). Throughout, heteroge-

neous decays were adequately fitted in terms of two lifetime components (see as an example F110S in Fig. 3). This analysis yielded an averaged lifetime ($\tau_{av} = \alpha_1\tau_1 + \alpha_2\tau_2$) of 0.076 s for F110S and 0.022 s for I7S . Thus, according to the triplet lifetime, both cavity mutants are more flexible in the central core of the protein harboring the phosphorescent probe.

The application of high pressure affects both the phosphorescence intensity and lifetime of each azurin species. It should be pointed out that when the protein unfolds, the phosphorescence lifetime falls to below detection limit and consequently the denatured fraction does not contribute to the phosphorescence emission of the sample. Thus, the intensity of phosphorescence extrapolated to time zero, P_0, when normalized by the fluorescence intensity F, P_0/F, is a direct measure of the native fraction of the protein population. For every protein, the pressure profile of P_0/F was found to be practically identical, within the ~5% precision of these measurements, to the fraction of azurin in the native state, $f_N = 1 - f_U$, as determined from the fluorescence f_U profiles of Fig. 2. This good correspondence between the native fraction of azurin determined by P_0/F and fluorescence indicates that the macromolecule is either fully native, with long-lived phosphorescence, or completely unfolded. Hence, even at denaturing pressures, there is no evidence of intermediate, partially structured conformations of the protein, that could be too flexible to be phosphorescent but with W48 still shielded from the solvent to fluoresce to the blue. The above correspondence between independent monitors of azurin denaturation supports the validity of a two-state unfolding equilibrium, meaning that in general unfolding proceeds from fully compact states.

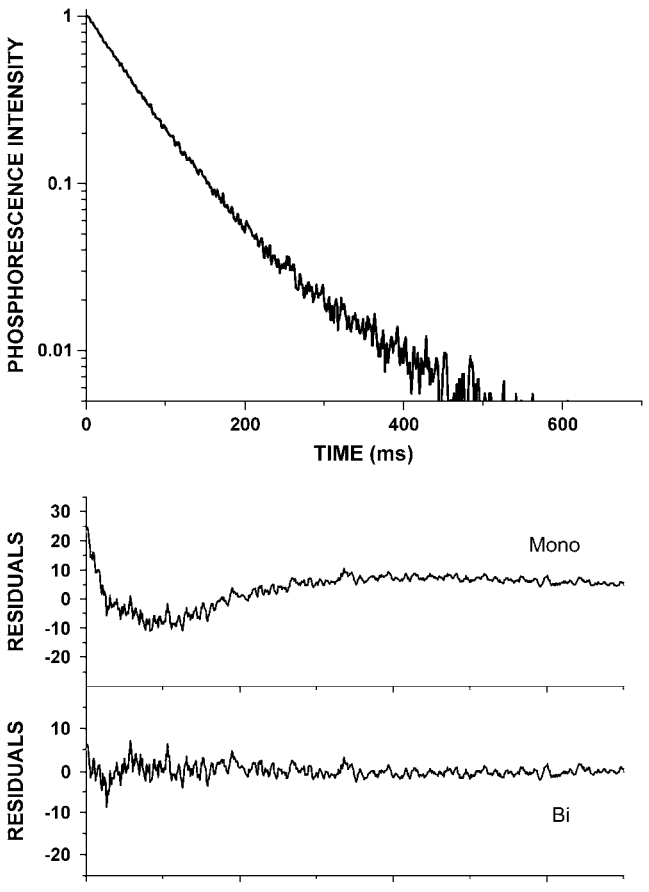

FIGURE 3 Trp phosphorescence decay of F110S azurin (1.4 μM) in 2 mM Tris-HCl, pH 7.5, at 40°C. The plots of residuals refer to mono- and biexponential fitting of the decay in buffer.

The pressure dependence τ_0 is reported for each protein in Fig. 4. Throughout, the pressure modulation of τ_0 was found to be a totally elastic process, as on decompression the change is promptly reversed. For the WT protein, we observe a biphasic τ profile characterized by an initial lengthening of the lifetime up to 3 kbar followed by its progressive reduction to values below τ_0. From the correlation between τ and the fluidity of the chromophore's environment (45), the pressure profile of τ attests to an initial tightening of the protein core, presumably owed to the preeminence of cavity reduction, followed by its progressive loosening in high pressure range, reflecting enhanced internal hydration.

The C3A/C26A azurin mutant behaves similarly to the WT protein. Although the much lower stability of the mutant relative to the WT limits the observation range to 3 kbar, τ is also found to increase, the compaction of the inner fold reaching its highest point on the same pressure range of the WT. This finding points out that despite the much smaller stability (6 kcal/mole) of C3A/C26A relative to WT, caused by the removal of the superficial disulphide link, hydration of the inner core and consequent loss of structural rigidity is as hindered as in the WT protein.

The introduction of a large cavity in proximity of W48 is expected to abate the rigidity of the local structure. The smaller τ_0 of F110S and I7S and the 3–4 orders of magnitude increase of the permeability of acrylamide to the protein core (30) confirm that cavity mutants are considerable more flexible than the WT. The response of protein dynamics to applied pressure will tell if the gain in flexibility of the cavity mutants is due to the presence of free voids or to the lubricating action of an internal water pools. Only in the former case would the macromolecules be highly compressible and pressure exert a drastic reduction of structural fluctuations. The flexibility changes inferred from τ (Fig. 4) show that for F110S, the initial compaction reaches a maximum at much lower pressure (1.5 kbar) than WT and C3A/C26A azurins, the trend reverting thereafter with a sizable twofold reduction of τ before reaching 3 kbar. For the more flexible cavity mutant, I7S, there is even no sign of compaction as the lifetime decreases monotonically above 0.5 kbar. In the latter, the triplet probe reports a sharp enhancement of protein flexibility at relatively low pressure, consistent with an overwhelming effect of internal protein hydration over any compaction of the structure. A similar behavior was also observed for the WT when approaching freezing temperatures where protein hydration is the dominant reaction to

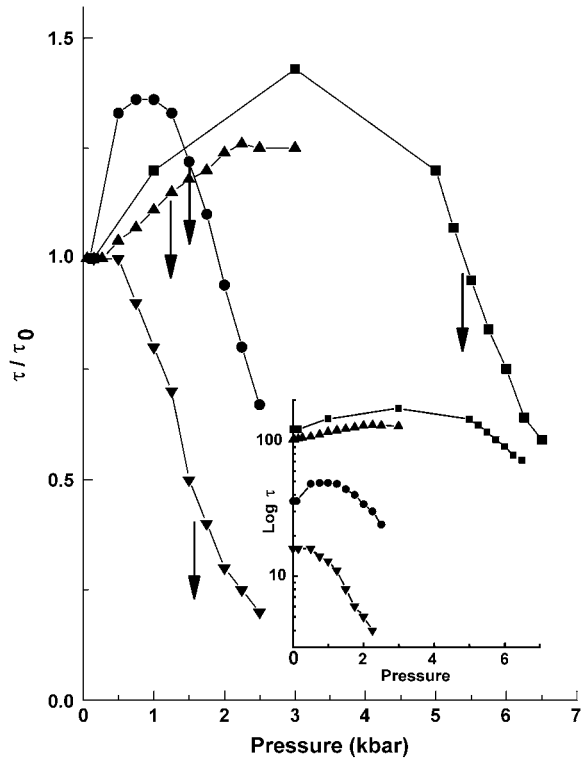

FIGURE 4 Pressure dependence of the phosphorescence lifetime (τ), normalized for its values at 1 bar, for azurin WT and mutant forms in Tris Cl 2 mM, pH 7.5, at 40°C. WT (■), F110S (●), I7S (▼), and C3A/C26A (▲). The absolute value of τ is shown in the inset. Arrows indicate the value of $P_{1/2}$, the pressure at which the protein sample is 50% denaturated.

pressurization (46). In either case, we do not observe the sharp tightening of conformational flexibility anticipated for empty cavities. Instead, the main response to pressure is consistent with the promotion of protein internal hydration. Hence, it appears that the new cavities of I7S and F110S are largely hydrated and that such a configuration confers high plasticity to the native state of azurin even at relatively low pressure. The lack of or decreased compaction of the inner core of cavity mutants with applied pressure points out that cavities are already filled with water, a finding that is consistent the invariance of $\Delta V°$ of the among the four azurin species.

The main conclusions to draw from the limited but homogeneous set of proteins examined is that the creation of an internal cavity will enhance the plasticity and lower the stability of the globular structure.

The possibility to discriminate between empty and water-filled cavities is also important for testing the validity of the relationship predicting the decrease in protein stability resulting from the creation of internal empty cavities. Based on a series of mutations in the core of phage T4 lysozyme, a correlation has been proposed (10,47) between $\Delta\Delta G$ and the size (ΔV) of the cavity created. According to this relationship, the energetic cost of making a cavity is linearly dependent on the volume of the created cavity plus an additional free-energy term determined by the difference in hydrophobicity of the two amino acid residues involved in the substitution. The cost of creating a cavity derives mostly from the missing van der Waals interactions between the side chain to be replaced and the surrounding atoms in the native structure and is estimated at ~0.022 kcal mole^{-1}Å^3 (10,47), a value frequently used in studies predicting protein stability (3,48). This $\Delta\Delta G$ versus ΔV relationship was found to hold in some cases (8,49) but data is also available that contrasts with it (3,50–52). In the case of I7S and F110S, the measured $\Delta\Delta G$ is ~6 kcal mole^{-1} for both mutants, and this value is fairly close to that predicted theoretically considering the substitution of Ile and Phe with a Ser plus the creation of cavity of the dimension calculated by x ray. However, we note that the agreement is totally fortuitous and misleading because the cavities are not empty but largely filled with water, and consequently $\Delta\Delta G$ should be much smaller. Both the difficulty in establishing the actual volume of a cavity, which depends on the shape of the cavity and the size of the probe used, and its variable extent of hydration suggest that ΔV is not a useful parameter for predicting free-energy changes in response to mutations. Moreover, buried water molecules in the interior of proteins can form a variety of hydrogen-bonded networks that can have a significant if unpredictable impact on protein stability (53,54).

The author is grateful to Dr. Giovanni Strambini for helpful discussions and for critical reading of the manuscript.

REFERENCES

1. Kellis, J. T., Jr., K. Nyberg, D. Sali, and A. R. Fersht. 1988. Contribution of hydrophobic interactions to protein stability. *Nature*. 333: 784–786.
2. Dill, K. A. 1990. Dominant forces in protein folding. *Biochemistry*. 29:7133–7155.
3. Adamek, D. H., L. Guerrero, M. Blaber, and D. L. Caspar. 2005. Structural and energetic consequences of mutations in a solvated hydrophobic cavity. *J. Mol. Biol.* 346:307–318.
4. Ernst, J. A., R. T. Clubb, H. X. Zhou, A. M. Gronenborn, and G. M. Clore. 1995. Demonstration of positionally disordered water within a protein hydrophobic cavity by NMR. *Science*. 267:1813–1817.
5. Matthews, B. W. 1993. Structural and genetic analysis of protein stability. *Annu. Rev. Biochem.* 62:139–160.
6. Matthews, B. W., A. G. Morton, and F. W. Dahlquist. 1995. Use of NMR to detect water within nonpolar protein cavities. *Science*. 270: 1847–1849.
7. Quillin, M. L., W. A. Breyer, I. J. Griswold, and B. W. Matthews. 2000. Size versus polarizability in protein-ligand interactions: binding of noble gases within engineered cavities in phage T4 lysozyme. *J. Mol. Biol.* 302:955–977.
8. Buckle, A. M., P. Cramer, and A. R. Fersht. 1996. Structural and energetic responses to cavity-creating mutations in hydrophobic cores: observation of a buried water molecule and the hydrophilic nature of such hydrophobic cavities. *Biochemistry*. 35:4298–4305.
9. Damjanovic, A., B. Garcia-Moreno, E. E. Lattman, and A. E. Garcia. 2005. Molecular dynamics study of hydration of protein interior. *Comput. Phys. Commun.* 169:126–129.
10. Eriksson, A. E., W. A. Baase, X. J. Zhang, D. W. Heinz, M. Blaber, E. P. Baldwin, and B. W. Matthews. 1992. Response of a protein structure to cavity-creating mutations and its relation to the hydrophobic effect. *Science*. 255:178–183.

11. Yu, B., M. Blaber, A. M. Gronenborn, G. M. Clore, and D. L. Caspar. 1999. Disordered water within a hydrophobic protein cavity visualized by x-ray crystallography. *Proc. Natl. Acad. Sci. USA.* 96:103–108.
12. Dwyer, J. J., A. G. Gittis, D. A. Karp, E. E. Lattman, D. S. Spencer, W. E. Stites, and E. B. Garcia-Moreno. 2000. High apparent dielectric constants in the interior of a protein reflect water penetration. *Biophys. J.* 79:1610–1620.
13. Otting, G., E. Liepinsh, B. Halle, and U. Frey. 1997. NMR identification of hydrophobic cavities with low water occupancies in protein structures using small gas molecules. *Nat. Struct. Biol.* 4:396–404.
14. Garcia, A. E., and G. Hummer. 2000. Water penetration and escape in proteins. *Proteins.* 38:261–272.
15. Vaitheeswaran, S., H. Yin, J. C. Rasaiah, and G. Hummer. 2004. Water clusters in nonpolar cavities. *Proc. Natl. Acad. Sci. USA.* 101:17002–17005.
16. Refaee, M., T. Tezuka, K. Akasaka, and M. P. Williamson. 2003. Pressure-dependent changes in the solution structure of hen egg-white lysozyme. *J. Mol. Biol.* 327:857–865.
17. Royer, C. A. 2002. Revisiting volume changes in pressure-induced protein unfolding. *Biochim. Biophys. Acta.* 1595:201–209.
18. Frye, K. J., C. S. Perman, and C. A. Royer. 1996. Testing the correlation between delta A and delta V of protein unfolding using m value mutants of staphylococcal nuclease. *Biochemistry.* 35:10234–10239.
19. Frye, K. J., and C. A. Royer. 1998. Probing the contribution of internal cavities to the volume change of protein unfolding under pressure. *Protein Sci.* 7:2217–2222.
20. Winter, R. 2002. Synchrotron X-ray and neutron small-angle scattering of lyotropic lipid mesophases, model biomembranes and proteins in solution at high pressure. *Biochim. Biophys. Acta.* 1595:160–184.
21. Gekko, K., and Y. Hasegawa. 1986. Compressibility-structure relationship of globular proteins. *Biochemistry.* 25:6563–6571.
22. Chalikian, T. V., M. Totrov, R. Abagyan, and K. J. Breslauer. 1996. The hydration of globular proteins as derived from volume and compressibility measurements: cross correlating thermodynamic and structural data. *J. Mol. Biol.* 260:588–603.
23. Kharakoz, D. P. 2000. Protein compressibility, dynamics, and pressure. *Biophys. J.* 79:511–525.
24. Mozhaev, V. V., K. Heremans, J. Frank, P. Masson, and C. Balny. 1996. High pressure effects on protein structure and function. *Proteins.* 24:81–91.
25. Cooper, A. 1976. Thermodynamic fluctuations in protein molecules. *Proc. Natl. Acad. Sci. USA.* 73:2740–2741.
26. Adman, E. T. 1991. Copper protein structures. *Adv. Protein Chem.* 42: 145–197.
27. Nar, H., A. Messerschmidt, R. Huber, M. van de Kamp, and G. W. Canters. 1991. Crystal structure analysis of oxidized Pseudomonas aeruginosa azurin at pH 5.5 and pH 9.0. A pH-induced conformational transition involves a peptide bond flip. *J. Mol. Biol.* 221:765–772.
28. Hammann, C., A. Messerschmidt, R. Huber, H. Nar, G.Gilardi, and G. W. Canters. 1996. X-ray crystal structure of the two site-specific mutants Ile7Ser and Phe110Ser of azurin from *Pseudomonas aeruginosa*. *J. Mol. Biol.* 255:362–366.
29. Mei, G., A. Di Venere, F. M. Campeggi, G. Gilardi, N. Rosato, F. De Matteis, and A. Finazzi-Agro. 1999. The effect of pressure and guanidine hydrochloride on azurins mutated in the hydrophobic core. *Eur. J. Biochem.* 265:619–626.
30. Cioni, P., E. de Waal, G. W. Canters, and G. B. Strambini. 2004. Effects of cavity-forming mutations on the internal dynamics of azurin. *Biophys. J.* 86:1149–1159.
31. Guzzi, R., L. Sportelli, C. La Rosa, D. Milardi, D. Grasso, M. P. Verbeet, and G. W. Canters. 1999. A spectroscopic and calorimetric investigation on the thermal stability of the Cys3Ala/Cys26Ala azurin mutant. *Biophys. J.* 77:1052–1063.
32. Cioni, P., and G. B. Strambini. 2002. Tryptophan phosphorescence and pressure effects on protein structure. *Biochim. Biophys. Acta.* 1595: 116–130.
33. Strambini, G. B., and E. Gabellieri. 1991. Phosphorescence from Trp-48 in azurin—influence of Cu(Ii), Cu(I), Ag(I), and Cd(Ii) at the coordination site. *J. Phys. Chem.* 95:4352–4356.
34. Strambini, G. B., and E. Gabellieri. 1996. Proteins in frozen solutions: Evidence of ice-induced partial unfolding. *Biophys. J.* 70:971–976.
35. Strambini, G. B., and E. Gabellieri. 1984. Intrinsic phosphorescence from proteins in the solid state. *Photochem. Photobiol.* 39:725–729.
36. Cioni, P., E. Bramanti, and G. B. Strambini. 2005. Effects of sucrose on the internal dynamics of azurin. *Biophys. J.* 88:4213–4222.
37. Hansen, J. E., D. G. Steel, and A. Gafni. 1996. Detection of a pH-dependent conformational change in azurin by time-resolved phosphorescence. *Biophys. J.* 71:2138–2143.
38. van de Kamp, M., M. C. Silvestrini, M. Brunori, J. Van Beeumen, F. C. Hali, and G. W. Canters. 1990. Involvement of the hydrophobic patch of azurin in the electron-transfer reactions with cytochrome C551 and nitrite reductase. *Eur. J. Biochem.* 194:109–118.
39. Gilardi, G., G. Mei, N. Rosato, G. W. Canters, and A. Finazzi-Agro. 1994. Unique environment of Trp48 in *Pseudomonas aeruginosa* azurin as probed by site-directed mutagenesis and dynamic fluorescence spectroscopy. *Biochemistry.* 33:1425–1432.
40. Bonander, N., J. Leckner, H. Guo, B. G. Karlsson, and L. Sjolin. 2000. Crystal structure of the disulfide bond-deficient azurin mutant C3A/C26A: how important is the S-S bond for folding and stability? *Eur. J. Biochem.* 267:4511–4519.
41. Strambini, G. B., B. A. Kerwin, B. D. Mason, and M. Gonnelli. 2004. The triplet-state lifetime of indole derivatives in aqueous solution. *Photochem. Photobiol.* 80:462–470.
42. Silva, J. L., and G. Weber. 1993. Pressure stability of proteins. *Annu. Rev. Phys. Chem.* 44:89–113.
43. Gonnelli, M., and G. B. Strambini. 1995. Phosphorescence Lifetime of Tryptophan in Proteins. *Biochemistry.* 34:13847–13857.
44. Gonnelli, M., and G. B. Strambini. 2005. Intramolecular quenching of tryptophan phosphorescence in short peptides and proteins. *Photochem. Photobiol.* 81:614–622.
45. Strambini, G. B., and M. Gonnelli. 1995. Tryptophan Phosphorescence in Fluid Solution. *J. Am. Chem. Soc.* 117:7646–7651.
46. Cioni, P., and G. B. Strambini. 1999. Pressure/temperature effects on protein flexibility from acrylamide quenching of protein phosphorescence. *J. Mol. Biol.* 291:955–964.
47. Xu, J., W.A. Baase, E. Baldwin, and B. W. Matthews. 1998. The response of T4 lysozyme to large-to-small substitutions within the core and its relation to the hydrophobic effect. *Protein Sci.* 7:158–177.
48. Hubbard, S. J., K. H. Gross, and P. Argos. 1994. Intramolecular cavities in globular proteins. *Protein Eng.* 7:613–626.
49. Takano, K., K. Ogasahara, H. Kaneda, Y. Yamagata, S. Fujii, E. Kanaya, M. Kikuchi, M. Oobatake, and K. Yutani. 1995. Contribution of hydrophobic residues to the stability of human lysozyme: calorimetric studies and X-ray structural analysis of the five isoleucine to valine mutants. *J. Mol. Biol.* 254:62–76.
50. Buckle, A. M., K. Henrick, and A. R. Fersht. 1993. Crystal structural analysis of mutations in the hydrophobic cores of barnase. *J. Mol. Biol.* 234:847–860.
51. Ratnaparkhi, G. S., and R. Varadarajan. 2000. Thermodynamic and structural studies of cavity formation in proteins suggest that loss of packing interactions rather than the hydrophobic effect dominates the observed energetics. *Biochemistry.* 39:12365–12374.
52. Vlassi, M., G. Cesareni, and M. Kokkinidis. 1999. A correlation between the loss of hydrophobic core packing interactions and protein stability. *J. Mol. Biol.* 285:817–827.
53. Wade, R. C., M. H. Mazor, J. A. McCammon, and F. A. Quiocho. 1991. A molecular dynamics study of thermodynamic and structural aspects of the hydration of cavities in proteins. *Biopolymers.* 31:919–931.
54. Takano, K., Y. Yamagata, S. Fujii, and K. Yutani. 1997. Contribution of the hydrophobic effect to the stability of human lysozyme: calorimetric studies and X-ray structural analyses of the nine valine to alanine mutants. *Biochemistry.* 36:688–698.